

# STUDY OF DUST PROPERTIES AROUND A WHITE DWARF IN INFRARED REGION

A Proposal

Submitted to the Department of Physics,  
Tri-Chandra Multiple Campus,  
Ghantaghar, Kathmandu,



By

Sanjay Rijal

August 31, 2021

## Abbreviations

**AGB:** Asymptotic Giant Branch

**EM:** Electromagnetic

**FIR:** Far Infrared

**Hz:** Hertz

**IR:** Infrared

**IRAS:** Infrared Astronomical Satellite

**ISM:** Interstellar Medium

**ISO:** Infrared Space Observatory

**JNPS:** Journal of Nepal Physical Society

**LOS:** Line of Sight

**MSX:** Midcourse Space Experiment

**SIMBAD:** Set of Identifications, Measurements and Bibliography for Astronomical Data

**FITS:** Flexible Image Transport System

**R.A.:** Right Ascension

**Dec.:** Declination

**WD:** White Dwarf

**WISE:** Wide-field Infrared Survey Explorer

## Abstract

During the asymptotic giant branch (AGB) phase, a major fraction of mass is spread by the stars ( $0.6 - 10 M_{\odot}$ ) in the interstellar medium (ISM) in the form of dust. In the left phase of Post-Main Sequence evolution, these dust are found to be surrounding the White Dwarf (WD). Some small fraction of dust is also formed in the circumstellar shells and cavities around WD which is usually a source of infrared (IR) excess. Formation and evolution of such IR dust structures are the results of high pressure events and such structures are crucial in the study of interaction phenomena in ISM. This research attempts to study isolated dust cavities around white dwarfs using Infrared Astronomical Satellite (IRAS) and AKARI surveys in the far IR region ( $60 \mu m$  and  $100 \mu m$ ). The study mainly focuses on the dust color temperature, dust mass, spectral emissivity, Jeans Mass along with their distribution and relations with each other.

**Keywords:** *White Dwarf, Infrared, Dust color temperature, Dust mass, Spectral emissivity, Jeans mass*

# Contents

<b>Abbreviations</b>	<b>ii</b>
<b>Abstract</b>	<b>iii</b>
<b>1 INTRODUCTION</b>	<b>1</b>
1.1 Background . . . . .	1
1.2 Objective . . . . .	2
1.3 Significance of the Project . . . . .	3
1.4 Scope of the Project . . . . .	3
<b>2 LITERATURE REVIEW</b>	<b>5</b>
<b>3 THEORY</b>	<b>8</b>
3.1 Dust Color Temperature Estimation . . . . .	8
3.2 Spectral Emissivity . . . . .	9
3.3 Visual Extinction and Optical Thickness . . . . .	10
3.4 Mass Estimation . . . . .	11
3.5 Jeans Criteria . . . . .	11
3.6 Inclination Angle . . . . .	12
<b>4 METHODOLOGY</b>	<b>14</b>
<b>5 EXPECTED OUTCOMES</b>	<b>16</b>
<b>Bibliography</b>	<b>17</b>

# Chapter 1

## INTRODUCTION

### 1.1 Background

Astrophysics is a branch of physics which is concerned with the application of methods and principles of physics to study astronomical objects and phenomena [1]. The emissions from the astronomical bodies are within the electromagnetic (EM) spectrum (below 1 Hz to  $10^{25}$  Hz) which are crucial in the study of various properties of the objects such as luminosity, temperature, density, mass, chemical composition, emissivity and so on. Most of the astronomical objects don't emit in the visible spectrum but the study of other spectral regions within the EM spectrum, especially IR spectrum (300 GHz – 430 THz), can be very useful for studying the properties and phenomena of such objects.

The observation and analysis of astronomical objects and phenomena using IR radiations is known as infrared astronomy. Frederick William Herschel, a German astrophysicist in early 1800, discovered IR light which became the foundation of infrared astronomy which began in the 1830s. All objects emit IR radiations which are detected by IR detectors. Some of the IR telescopes that have been operating in space are: Infrared Astronomical Satellite (IRAS), Infrared Space Observatory (ISO), Midcourse Space Experiment (MSX), Spitzer Space Telescope, Akari, Herschel Space Observatory and Wide-field Infrared Survey Explorer (WISE). The IR data obtained from the surveys of these detectors are processed and analyzed to study the astronomical objects and phenomena.

Before the 20th century, the Milky Way galaxy was thought to consist of stars in a vacuum. The first observational evidence that there was a general ISM between stars came from the photographic

spectroscopy of spectroscopic binary stars in the early 20th century. Interstellar Medium (ISM) is the matter as well as radiation existing between the stellar systems or simply ISM is anything not in stars [2]. ISM primarily consists of Hydrogen (91%) followed by Helium (8.9%) with trace amounts of other gases (0.1%) like Carbon, Oxygen and Nitrogen [3]. Hydrogen and Helium are mainly the result of primordial nucleosynthesis while other metals (elements heavier than Hydrogen and Helium) are the consequence of stellar evolution processes. These gases in ISM exist in a number of thermal phases depending on the local conditions of ionization, heating and so on. In all phases, ISM has extremely low density. In cool, dense regions of ISM, matter is mainly found in molecular forms with density upto  $10^6$  molecules per  $\text{cm}^3$  while in hot, diffuse regions, matter are mostly in ionized state with density as low as  $10^{-4}$  ions per  $\text{cm}^3$ . By mass, ISM is composed of 99% gases and 1% dust [4]. Stars form within the dense regions of ISM contributing to the molecular clouds, which is a type of interstellar cloud, the density and size of which results in formation of molecules mostly  $\text{H}_2$ . These molecular clouds plenish the ISM with matter as well as energy through planetary nebulae, stellar winds, supernovae and so on. This interaction between stars and ISM helps in determining the rate of depletion of gaseous contents of a galaxy and hence its lifespan of active star formation. Molecular clouds are in contrast to other regions of ISM which contain predominantly ionized gases.

On the other hand, even though ISM contains only 1% of dust, they play a crucial role in determining the chemical as well as thermodynamic distribution of ISM. These dusts are generally solid microscopic particles of silicate, graphites, ice and carbon bearing compounds like hydrocarbons. They are usually  $0.1 - 1 \mu\text{m}$  in size. They are generally formed in the shells around evolved stars in AGB stages in stellar evolution while some fraction in circumstellar shells around super giants, planetary nebulae and white dwarfs. The majority of dust is formed in the cool, dense regions of ISM by the process of accretion and coagulation while many other processes are still unknown [5].

## 1.2 Objective

The objectives of the project can be divided as:

### General Objective

- To study the properties of dust structures around possible white dwarf candidates and the

ongoing astrophysical phenomena.

### Specific Objectives

- To evaluate and analyze the IR flux, dust color temperature, visual extinction and dust mass around the possible white dwarf candidates.
- To study three dimensional structure by studying the inclination angle of various internal parts of the dust structure.
- To predict whether the structure around is a probable star forming region or not through the analysis of Jeans criteria.

## 1.3 Significance of the Project

The project has various significances, some of which are as follows:

- The dust properties around White Dwarf can preserve the record of fossils of the parent star and can also reveal the prehistoric information helping light up the stellar evolution.
- The study of dust is also important to explore the chemistry of ISM. Infrared spectroscopy reveals the ongoing chemical as well as physical processes in ISM.
- Dust structures absorb the high energy radiation, like Ultraviolet, from the hot region of ISM and re-radiate the absorbed radiation as IR radiation. This implies that dust structures are important components in regulating the heating mechanism in ISM. Therefore, the study of dust grain is essential to understand the thermal distribution in ISM.
- Interstellar dust consists of Silicates and Carbon compounds which are the fundamental components for the formation of planetary systems, like the solar system. So, the study of such dust structures can provide crucial information regarding the evolution of the planetary systems.

## 1.4 Scope of the Project

The project explores the infrared data obtained from the IRAS and AKARI surveys at 60  $\mu\text{m}$  and 100  $\mu\text{m}$  to evaluate and analyze the properties of the dust structure around candidate white

dwarfs. These properties include dust color temperature, dust mass, IR flux, inclination angle, visual extinction and Jeans mass. However, the project doesn't encompass the following areas:

- The project cannot predict the exact stellar evolution model as the calculation of nature of the perturbation in the surroundings are required to predict the exact model of stellar formation.
- The thermal properties of the dust within the selected regions along with the black body spectrum within dust clumps do not comply with the area of the study.
- The multiwavelength properties of dust structures cannot be studied using IR data.



## Chapter 2

# LITERATURE REVIEW

A.K Gautam and B. Aryal [6] in 2019 studied the dust color temperature and visual extinction distribution of an FIR cavity at 60 and 100  $\mu\text{m}$  IRAS map using SkyView Virtual Observatory. The study was focused around an AGB star located at R.A. (J2000) =  $01^h 41^m 01^s$  and Dec (J2000) =  $71^\circ 04' 00''$  with a cavity structure at R.A. (J2000) =  $01^h 46^m 57.2^s$  and DEC (J2000) =  $71^\circ 24' 57.1''$ . From the flux distribution, the average temperature of the cavity was found to be 22.2 K with dust color temperature range of  $(19.7 \pm 0.65)$  K to  $21.1 \pm 0.35$  K which suggested the cavity was isolated and stable. Further such low offset temperature implied symmetric outflow or symmetric distribution of temperature and density and the particles were vibrating independently. They estimated the mass of the cavity to be  $0.0094 M_\odot$ . The distribution of dust mass depicted that the minimum temperature region was denser situated at the maximum mass region in the selected contour which is a usual trend. They concluded that distribution of mass was in accordance with the cosmological principle. Regarding the relation between visual extinction and dust color temperature which was obtained as linear they concluded a systematic trend (i.e visual extinction decreases with increase in dust color temperature and vice-versa).

A research paper published in Journal of Nepal Physical Society (JNPS) by A.K Gautam and D.N Chhatkuli [7] in 2020 focused on the Planck function distribution in the FIR cavity around AGB2308+6058, an AGB star. The star was close to the Galactic plane at a galactic latitude of  $0.6^\circ$  resulting in a strong radiation field. The dust color temperatures were estimated within the range  $22.76 \pm 0.14$  K to  $23.55 \pm 0.29$  K with a low offset of 0.79 K suggesting thermodynamic equilibrium in the cavity. The average temperature of the cavity was noted to be 22.14 K. A fluctuation in the

distribution of Planck function along both diameters of the FIR cavity was noticed, suggesting that the dust particles were oscillating non-uniformly and independently. Further, the dust mass was estimated as  $0.129 M_{\odot}$  with contour maps showing greater mass densities in the low temperature regions thus supporting the cosmological principle. Also, the relation between visual extinction and dust color temperature which was found to be linear with high negative degree of correlation.

A similar study was done by A.K. Jha and B. Aryal [8] in 2018 regarding the dust color temperature estimation of two FIR cavities located at R.A. (J2000) =  $14^h 41^m 23^s$  14 h 41 m 23 s, Dec. (J2000) =  $64^{\circ} 04' 17''$  and R.A. (J2000) =  $05^h 05^m 35^s$ , Dec. (J2000) =  $69^{\circ} 35' 25''$  using IRAS (60 and  $100 \mu\text{m}$ ) and AKARI (90 and  $140 \mu\text{m}$ ) surveys. The dust color temperature of first cavity located close to the galactic plane was found to lie in the range  $23.4 \pm 1.3 \text{ K}$  to  $24.1 \pm 1.4 \text{ K}$  with an offset of  $0.7 \text{ K}$  in IRIS maps while  $26.0 \pm 1.5 \text{ K}$  to  $28.2 \pm 1.6 \text{ K}$ , with an offset of  $2.2 \text{ K}$  in AKARI map. Similarly for second cavity far from the galactic plane, temperature ranges were  $22.2 \pm 1.2 \text{ K}$  to  $24.6 \pm 1.3 \text{ K}$ , with an offset of about  $2.4 \text{ K}$  and  $25.4 \pm 1.4 \text{ K}$  to  $29.7 \pm 1.7 \text{ K}$ , with a larger offset of  $4.3 \text{ K}$  in IRAS and AKARI maps respectively. Low offset suggested a higher probability of local thermodynamic equilibrium. Further the difference in offset values of IRAS and AKARI suggested non-uniformity of the Planck function in the second cavity which led to the conclusion that the temperature of the second cavity may vary within the mean free path of the dust which causes deviation from the local thermodynamic equilibrium.

Another research done by A.K Jha and B. Aryal [9] on the pulsar wind driven structure in FIR IRAS map located at a latitude of  $-10^{\circ}$  was focused on studying the flux variation, temperature and mass profile of an isolated deep cavity. The temperature of the cavity was found within the range of  $29.28 \text{ K}$  to  $23.4 \text{ K}$  with a offset of about  $6 \text{ K}$  which is a high offset that leads to the conclusion that the cavity is either dip or might be formed due to various processes like interstellar bubble formation, dust and grain formation and so on. Moreover, the mass of the cavity was estimated to be around  $0.0013 M_{\odot}$  with a mass deficit per pixel of  $2.52 \times 10^{24} \text{ Kg}$  resulting in the energy of the pulsar to expel the mass to be  $5.04 \times 10^{36} \text{ J}$ .

“Study of Dust Cavity around the White Dwarf WD 0352-049 in Infrared Astronomical Satellite Map”, a research article published by M.S. Paudel and et al [10] in 2021 in JNPS presented research work on FIR images of a dust cavity around WD 0352-049 using SkyView Virtual Observa-

tory. The study involved flux density, dust color temperature and dust mass estimation. According to the study, the temperature of the whole cavity was estimated within the range of  $24.09 \pm 0.50$  K to  $21.87 \pm 0.61$  K with a fluctuation of 2.22 K and an average value of  $23.09 \pm 1.11$  K. The offset temperature less than 5 K suggested that the dust in the cavity structure was less disturbed from external radiation sources and evolving independently while the average temperature led to the conclusion the dust is not a Cirrus-type cloud. The Gaussian distribution of the dust color temperature was visualized as well, suggesting the local thermodynamic equilibrium. Also, the variation of flux and temperature along both the axes indicated the presence of thermal wind due to the WD near the center of the cavity. The study of Jean's criteria of the structure depicted the possibility of star formation activity within the structure and that of inclination angle concluded that the structure is uniformly shaped and regularly structured from the morphological point of view.

# Chapter 3

## THEORY

### 3.1 Dust Color Temperature Estimation

The dust temperature ( $T_d$ ) in each pixel of an FIR image can be obtained by considering the dust in a single beam is isothermal and that the observed ratio of 60 to 100  $\mu\text{m}$  emission is the result of blackbody radiation from the dust grains at  $T_d$  modified by a power-law emissivity spectral index (beta). The flux density of emission at wavelength  $\lambda_i$  is given by [11],

$$F_i = \left[ \frac{2hc}{\lambda_i^3 (e^{\frac{hc}{\lambda_i kT}} - 1)} \right] N_d \alpha \lambda_i^{-\beta} \Omega_i \quad (3.1)$$

where  $N_d$  represents column density of dust grains,  $\alpha$  is a constant that relates the flux to the optical depth of the dust and  $\Omega_i$  is the solid angle subtended at  $\lambda_i$  by the detector.

With the assumptions that the dust emission is optically thin at 60  $\mu\text{m}$  and 100  $\mu\text{m}$  (i.e.  $\tau_d \ll 1$ ) and that  $\Omega_{60} \approx \Omega_{100}$  (true for IRIS image), we can write the ratio,  $R$ , of the flux densities at 60  $\mu\text{m}$  and 100  $\mu\text{m}$  as,

$$R = \frac{F_{60}}{F_{100}} = \left[ \frac{60}{100} \right]^{-(3+\beta)} \left[ \frac{e^{\frac{T_{100}}{T_d}} - 1}{e^{\frac{T_{60}}{T_d}} - 1} \right] \quad (3.2)$$

Using the relation,  $T_{100} = \frac{hc}{\lambda_{100} \cdot k_B}$  and  $T_{60} = \frac{hc}{\lambda_{60} k_B}$  we get,  $T_{100} = 144K$  and  $T_{60} = 240K$ . Also, 1 can be dropped from both numerator and denominator of equation 3.2 for smaller values of T. So,

$$R = 0.6^{-(3+\beta)} \left[ \frac{e^{\frac{144}{T_d}}}{e^{\frac{240}{T_d}}} \right] \quad (3.3)$$

Taking natural logarithm of equation 3.3 we obtain the value of  $T_d$  as,

$$T_d = \frac{-96}{\ln\{R \times 0.6^{(3+\beta)}\}} \quad (3.4)$$

For AKARI FIR data at 90  $\mu m$  and 140  $\mu m$ , equation 3.2 can be written as,

$$R = \frac{F_{90}}{F_{140}} = \left[ \frac{90}{140} \right]^{-(3+\beta)} \left[ \frac{e^{\frac{T_{140}}{T_d}} - 1}{e^{\frac{T_{90}}{T_d}} - 1} \right] \quad (3.5)$$

Using the relation,  $T_{140} = \frac{hc}{\lambda_{140} \cdot k_B}$  and  $T_{90} = \frac{hc}{\lambda_{90} k_B}$  we get,  $T_{140} = 103K$  and  $T_{90} = 160K$ . Also, 1 can be dropped from both numerator and denominator of equation 3.5 for smaller values of T. So,

$$R = 0.64^{-(3+\beta)} \left[ \frac{e^{\frac{103}{T_d}}}{e^{\frac{160}{T_d}}} \right] \quad (3.6)$$

Taking natural logarithm of equation 3.6 we obtain the value of  $T_d$  as,

$$T_d = \frac{-57}{\ln\{R \times 0.6^{(3+\beta)}\}} \quad (3.7)$$

## 3.2 Spectral Emissivity

According to Dupac and et al.[12], the inverse relation between the emissivity index  $\beta$  and dust color temperature  $T_d$  is,

$$\beta = \frac{1}{\delta + \omega T_d} \quad (3.8)$$

where parameters  $\delta$  and  $\omega$  depend on the dust grain properties like composition, size, compactness and so on and have values  $\delta = 0.40 \pm 0.02$  and  $\omega = 0.0079 \pm 0.0005 K^{-1}$

For pure black body,  $\beta = 0$ ,

For amorphous layer-lattice matter,  $\beta \sim 1$  and

For metals and crystalline dielectrics  $\beta \sim 2$ .

### 3.3 Visual Extinction and Optical Thickness

Considering the fact that the dust is optically very thin i.e.:  $\tau_d \ll 1$ , we can calculate the dust optical depth at 100  $\mu\text{m}$  as [13],

$$\tau_{100} = \frac{F_\lambda(100\mu\text{m})}{B_\lambda(\lambda, T_d)} \quad (3.9)$$

where  $F_\lambda(100)$  is the observed flux at wavelength of 100  $\mu\text{m}$  and  $B_\lambda(\lambda, T_d)$  is the plank function given by,

$$B_\lambda(\lambda, T) = \frac{2hc^2}{\lambda^5} \left[ \frac{1}{e^{\frac{hc}{\lambda k_B T}} - 1} \right] \quad (3.10)$$

is the spectral emissive power per unit area per unit solid angle for a particular wavelength of radiation.

Interstellar extinction is the dimming of distant objects due to the presence of dust in the ISM along the line of sight (LOS). The visual extinction can be defined as the difference between the magnitude with and without the interstellar extinction and is expressed as,

$$A(\lambda) = m_{\text{attenuated}} - m_0 = 2.5 \log_{10} \left[ \frac{F_\lambda^0}{F_\lambda^a} \right] \quad (3.11)$$

Where,  $F_\lambda^a$  is the dust attenuated observed flux and  $m_{\text{attenuated}}$  is corresponding apparent magnitude of the object, and  $F_\lambda^0$  is the flux that would have been observed if there would have been no attenuation from dust and  $m_0$  is corresponding apparent magnitude of the object. Let the optical thickness be  $\tau(\lambda)$ , then

$$F_\lambda^a = F_\lambda^0 e^{-\tau(\lambda)} \quad (3.12)$$

Combining equations 3.11 and 3.12 we obtain,

$$A(\lambda) = (2.5 \log_{10} e) \tau(\lambda) \quad (3.13)$$

The relation between extinction and optical thickness is linear with slope  $(2.5 \log_{10} e)$  [11]. This equation gives very high value of optical thickness for 100  $\mu\text{m}$  and 140  $\mu\text{m}$  wavelength which doesn't comply with our assumption that the dust are optically thin for 100  $\mu\text{m}$  and 140  $\mu\text{m}$  wavelength. Assuming optically thin emission, the value of V - band extinction is as modified by Wood et. al [13] for 100  $\mu\text{m}$  flux is given by,

$$A(\lambda) = 15.078(1 - e^{\frac{-\tau_{100}}{641.3}}) \quad (3.14)$$

### 3.4 Mass Estimation

First the value of flux density,  $F_\lambda$ , at 100  $\mu\text{m}$  is determined then the dust mass can be calculated as [14],

$$M_d = \frac{4a\rho}{3Q_\lambda} \left[ \frac{F_\lambda D^2}{B_\lambda(\lambda, T)} \right] \quad (3.15)$$

where  $a$  = weighted grain size (0.1  $\mu\text{m}$ )

$\rho$  = grain density (3000  $\text{kg m}^3$ )

$Q_\lambda$  = grain emissivity at wavelength  $\lambda$  (0.001 for 100  $\mu\text{m}$ )

$B_\lambda(\lambda, T)$  = Planck's function

substituting the values we get the reduced equation as suggested by Young and et al [15],

$$M_d = 0.4 \left[ \frac{F_\lambda D^2}{B_\lambda(\lambda, T)} \right] \quad (3.16)$$

FIR emission is measured from the 100  $\mu\text{m}$  IRAS images for the derivation of the dust mass because the longer wavelength measurements give us more precise dust masses due to the characteristics of the Planck function.

### 3.5 Jeans Criteria

According to the Virial theorem, the kinetic energy  $\langle T \rangle$  of a stable system must be equal to the negative half of its gravitational potential energy  $\langle U \rangle$ . Mathematically, it is expressed as,

$$\langle 2T \rangle + \left\langle \sum_{i=1}^n F_i, r_i \right\rangle = 0 \quad (3.17)$$

Since  $\left\langle \sum_{i=1}^n F_i, r_i \right\rangle = \langle U \rangle$  so,

$$\langle 2T \rangle = -\frac{1}{2} \langle U \rangle \quad (3.18)$$

It implies that there must exist a critical mass of a molecular cloud to be stable or to collapse. The process of collapsing of a molecular cloud due its own gravity is known as gravitational collapse. For the cloud to be stable, it must be in hydrostatic equilibrium. If the internal pressure of the gas

is greater than the gravitational force then the mass will collapse and instability occurs which is known as Jeans instability. Jeans mass, named after British physicist James Jeans, is the critical mass required for the Jeans stability. It depends on two thermodynamic parameters; pressure (P) and density ( $\rho$ ) [16]. The relation can be expressed as,

$$M \propto P^a \rho^b G^c \quad (3.19)$$

where G = universal gravitational constant and a, b, c are constants to be determined. On determining the values of a, b, c using dimensional method we get Jeans mass as,

$$M_J = \frac{K P^{\frac{3}{2}}}{\rho^2 G^{\frac{3}{2}}} \quad (3.20)$$

where K is proportionality constant which depends on the nature of perturbation. The perturbation depends on the speed of acoustic waves and adiabatic index.

For slow varying perturbation,

$$K = \frac{4}{3} \pi^{\frac{5}{2}} \quad (3.21)$$

From equation 3.20 Jeans length  $\lambda_J$  can also be calculated as,

$$\lambda_J = \left[ \frac{\pi k_B T}{\mu m_H G \rho} \right]^{\frac{1}{2}} \quad (3.22)$$

where  $k_B$  = Boltzmann's constant

T = temperature of the molecular cloud

$\mu$  = mass per particle in the cloud

$m_H$  = mass of proton (in kg)

Jeans length gives the critical size of the cloud at a given temperature for Jeans stability.[17]

## 3.6 Inclination Angle

The inclination angle (i) is the angle between the LOS and the normal vector of the plane of the structure. This can be estimated by using Holmberg [18] formula,

$$\cos^2 i = \frac{\left(\frac{b}{a}\right)^2 - q^{*2}}{1 - q^{*2}} \quad (3.23)$$



where,  $(b/a)$  is the ratio of minor to major diameter and  $q^*$  is the intrinsic flatness of the structure. The intrinsic flatness is closely related to nebula morphology. It depends on the amount of molecular hydrogen and the dust. The dust grains obtain energy from the heating due to photoelectric effect and low-energy cosmic rays. Due to this vibrational degree of freedom is greatly enhanced. This makes the cloud to be flat (opening angle gradually increase with the dilution and vibrational excitation of the dust). Thus the range of the intrinsic flatness of the cloud is taken between 0.13 to 0.33. [19]

# Chapter 4

## METHODOLOGY

The following steps are planned to be adopted throughout the project.

- Search the catalogue of White Dwarfs from literature and use it to carry systematic search in SkyView Virtual Observatory along with Simbad Astronomical Database.
- Select the few clearly isolated regions around White Dwarf in infrared wavelength.
- Use the FITS image of selected regions to find the infrared flux using Aladin.
- Extract the IR flux values of each pixel within the region of interest and process the data to study the distribution of flux, dust color temperature, dust mass, gas mass, density, Planck's function using Python.
- Use appropriate statistical methods for the analysis of the results.

The overall research plan flow chart is as shown in the figure 4.1.

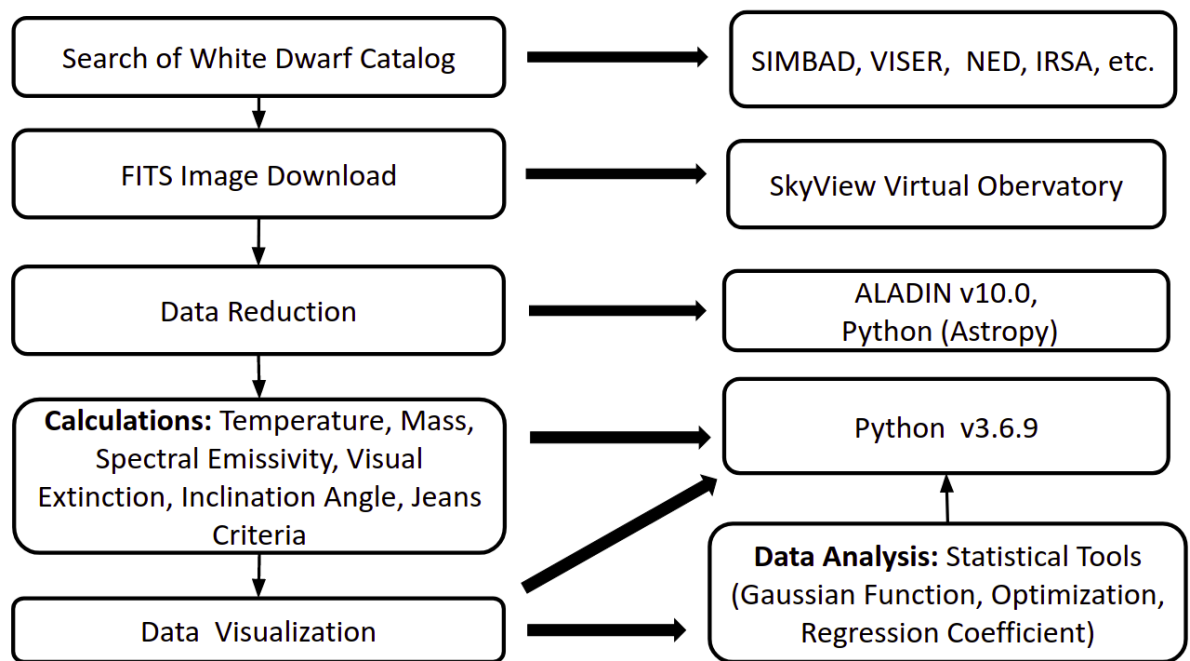


**Figure 4.1:** Methodology (Research Plan)

# Chapter 5

## EXPECTED OUTCOMES

The following results are expected from the project work.

- The temperature of the dust structure is expected within the range of 10K - 100K. However, some fluctuations might occur as a result of some radiative sources in the background.
- ISM is a very low density region of space so, the density of the dust in the region of interest is expected to be less than  $10^{-15} \text{ kg m}^{-3}$ .
- For the structure formation in the ISM the total mass of the dusts and gases must be greater than the Jeans mass of the region. For the effectiveness of the region, the mass of the dust structure with gas is expected to be greater than the Jeans mass.
- It is also expected that there exists some relation between the dust temperature and mass which could also be affected by the size of the dust clumps.

# Bibliography

- [1] Dan Maoz. *Astrophysics in a Nutshell*, volume 16. Princeton university press, 2016.
- [2] Donald E Osterbrock. A fortunate life in astronomy. *Annual Review of Astronomy and Astrophysics*, 38(1):1–33, 2000.
- [3] Katia M Ferriere. The interstellar environment of our galaxy. *Reviews of Modern Physics*, 73(4):1031, 2001.
- [4] F Boulanger, P Cox, and AP Jones. Dust in the interstellar medium. In *Astronomie spatiale infrarouge, aujourd’hui et demain Infrared space astronomy, today and tomorrow*, pages 251–335. Springer, 2000.
- [5] Alexander GGM Tielens. *The physics and chemistry of the interstellar medium*. Cambridge University Press, 2005.
- [6] AK Gautam and B Aryal. Study of dust color temperature and visual extinction distribution of a far infrared cavity at 60 and 100  $\mu\text{m}$  iras map around the agb star at galactic latitude 8.6 . *BIBECHANA*, 17:42–49, 2020.
- [7] AK Gautam and DN Chhatkuli. Planck function distribution in the far infrared cavity nearby agb star at galactic latitude 0.6  $^{\circ}$ . *Journal of Nepal Physical Society*, 6(2):97–103, 2020.
- [8] AK Jha and B Aryal. Dust color temperature distribution of two fir cavities at iris and akari maps. *Journal of Astrophysics and Astronomy*, 39(2):1–7, 2018.
- [9] Ajay Kumar Jha and Binil Aryal. A study of a pulsar wind driven structure in far-infrared iras map at lattitude-10 $^{\circ}$ . *Journal of Institute of Science and Technology*, 22(1):1–9, 2017.

- [10] MS Paudel, P Bhandari, and S Bhattarai. Study of dust cavity around the white dwarf wd 0352-049 in infrared astronomical satellite map. *Journal of Nepal Physical Society*, 7(2):110–118, 2021.
- [11] Scott L Schnee, Naomi A Ridge, Alyssa A Goodman, and Jason G Li. A complete look at the use of iras emission maps to estimate extinction and dust temperature. *The Astrophysical Journal*, 634(1):442, 2005.
- [12] Xavier Dupac, J-P Bernard, N Boudet, M Giard, J-M Lamarre, C Mény, F Pajot, I Ristorcelli, G Serra, B Stepnik, et al. Inverse temperature dependence of the dust submillimeter spectral index. *Astronomy & Astrophysics*, 404(1):L11–L15, 2003.
- [13] D. O. Wood D. A. Daugherty and P. C. Myers. Iras images of nearby dark clouds. *Astrophysics Journal and Supplement Series*, 95:457–501, 1994.
- [14] Roger H Hildebrand. The determination of cloud masses and dust characteristics from sub-millimetre thermal emission. *Quarterly Journal of the Royal Astronomical Society*, 24:267, 1983.
- [15] K Young, TG Phillips, and GR Knapp. Circumstellar shells resolved in iras survey data. ii-analysis. *The Astrophysical Journal*, 409:725–738, 1993.
- [16] B.W. Carroll and D.A. Ostlie. *An Introduction to Modern Astrophysics*. Pearson Education Limited, 2nd edition.
- [17] Hannu Karttunen, Pekka Kröger, Heikki Oja, Markku Poutanen, and Karl Johan Donner. *Fundamental astronomy*, volume 4. Springer, 2007.
- [18] E. Holmberg. Investigations of the systematic errors in the apparent diameters of the nebulae. 117.
- [19] M. P. Haynes R. Giovanelli. *Astronomical Journal*, 896, 1984.